Received: 7 June 2020 | Accepted: 26 November 2020

DOI: 10.1002/pamm.202000041

An RVE-based investigation of thermoplastic vulcanizates exemplified by EPDM/PP

Wanrong Sun[1,*] and **Daniel Juhre**[1]

[1] Institute of Mechanics, Otto von Guericke University, 39106 Magdeburg, Germany

In this contribution, the material behaviour of thermoplastic vulcanizate is investigated using the example of ethylene-propylene-diene monomer rubber (EPDM) and polypropylene (PP). For modelling of viscoelastic effects, the generalized Maxwell element is applied, whereby the isochoric stresses of parallel Maxwell elements are determined via evolution equations. In order to take the morphological composition of TPV into account, a representative volume element (RVE) consisting of PP as matrix and EPDM as included material is considered. In a following numerical example, a cyclic shear test is presented, where the resulting force and stress distribution is evaluated. Thus, the results show the macroscopic material behaviour under the consideration of microstructure.

1 Introduction

Thermoplastic vulcanizates (TPV) are used in a wide range of applications such as medical technologies, automotives and consumer goods. They are characterized by a good combination of the individual material properties. Furthermore, existing manufacturing technologies can be used to produce goods. TPV belongs to the group of thermoplastic elastomers (TPE). With respect to the morphological composition, a soft cross-linked elastomer phase (dispersed phase) is embedded in a hard thermoplastic phase (matrix). The morphology has a significant influence on the macroscopic material behaviour, which can be seen for example by the appearance of hysteresis responses under cyclic load. In this context, the macroscopic material behaviour is investigated under the consideration of microstructure using the representative volume element technique consisting of EPDM/PP.

2 Governing Equations

In this section, the fundamentals for the phenomenological description of viscoelastic effects of thermoplastic vulcanizates are described. For modelling of the component material behaviour, an incompressible hyperelastic Neo-Hooke material is assumed, so the strain energy Ψ can be additively decomposed into a volumetric U and isochoric $\hat{W}$ part according to

$$\begin{aligned} \Psi &= U(J) + \hat{W}\left(\hat{\boldsymbol{C}}\right) \\ \Psi &= \underbrace{\frac{K}{4}\left(J^2-1\right) - \frac{K}{2} ln\left(J\right)}_{volumetric\, part} + \underbrace{\frac{\mu}{2}\left(I_{\hat{\boldsymbol{C}}} - 3\right)}_{isochoric\, part} \quad . \end{aligned} \tag{1}$$

Therein K and μ are equal to the compression modulus and shear modulus, $J = det\left(\boldsymbol{F}\right)$ is the determinant of deformation gradient $\boldsymbol{F}$ and $I_{\hat{\boldsymbol{C}}} = tr\left(J^{-2/3}\boldsymbol{C}\right)$ is the first invariant of isochoric right Cauchy-Green tensor. With knowledge of the strain energy, the constitutive law

$$\begin{aligned} \boldsymbol{S} &= 2\frac{\partial \Psi}{\partial \boldsymbol{C}} = \boldsymbol{S}^{vol} + \boldsymbol{S}^{iso} \\ \boldsymbol{S} &= \frac{K}{2}\left(J^2-1\right)\boldsymbol{C}^{-1} + \mu J^{\frac{2}{3}}\left[\boldsymbol{1} - \frac{1}{3} tr\left(\boldsymbol{C}\right)\boldsymbol{C}^{-1}\right] \end{aligned} \tag{2}$$

can be determined, where $\boldsymbol{S}$ is the second Piola-Kirchhoff stress with its volumetric $\boldsymbol{S}^{vol}$ and isochoric $\boldsymbol{S}^{iso}$ parts.

Afterwards, the rheological model for modelling of viscoelastic effects is discussed. The generalized Maxwell element, according to Fig. 1, is applied, which consists of a single spring with parallel Maxwell elements. The corresponding stresses and evolution equations are summarized in Eq. 3 - 5.

* Corresponding author: e-mail wanrong.sun@ovgu.de, phone +49 391 67 52886

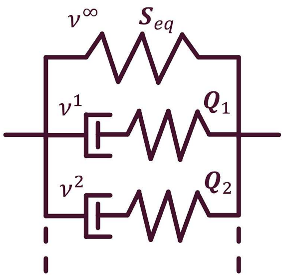

Fig. 1: Generalized Maxwell element

$$\boldsymbol{S} = \boldsymbol{S}_{eq}^{vol} + \nu^\infty \boldsymbol{S}_{eq}^{iso} + \Sigma_{i=1}^{n} \nu^i \boldsymbol{Q}_{neq,i}^{iso} \tag{3}$$

$$\dot{\boldsymbol{Q}}_{neq,i} + \frac{1}{\tau_i} \boldsymbol{Q}_{neq,i} = \dot{\boldsymbol{S}}_{eq}^{iso} \tag{4}$$

$$1 = \nu^\infty + \Sigma_{i=1}^{n} \nu^i \tag{5}$$

Eq. 3 describes the viscoelastic material behaviour, where the influence of parallel Maxwell elements is weighted by the factor ν^i and superimposed to the equilibrium stress $\boldsymbol{S}_{eq}^{iso}$. Within the evolution equation, see Eq. 4, $\boldsymbol{Q}_{neq,i}$ represents the isochoric stress at Maxwell element, τ_i the corresponding relaxation parameter and $\dot{\boldsymbol{S}}_{eq}^{iso}$ the time derivation of the isochoric second Piola-Kirchhoff stress of single spring. The time derivative is achieved by using a backward difference scheme.

3 Results

The investigated RVE is shown in Fig. 2 and the corresponding material properties are summarized in Tab. 1. The filling material is located at the corners and out of centre of the element. Thus the RVE has non-symmetrical mass distribution. With respect to the boundary conditions, it is assumed that the lower end of the RVE is fixed and cyclic displacements are predefined at the upper end. Furthermore, periodic boundary conditions are applied at the lateral edges.

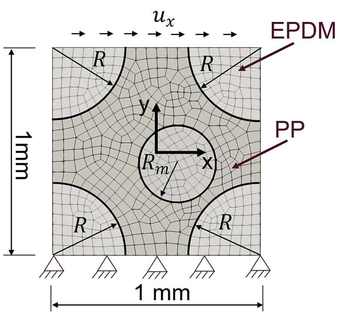

Fig. 2: RVE-model

Property	Name	value
Bulk modulus PP	K_{PP}	1190.5 MPa
Shear modulus PP	G_{PP}	174.8 MPa
Relaxation time PP	τ_{PP}	0.5
Bulk modulus EPDM	K_{EPDM}	26.3 MPa
Shear modulus EPDM	G_{EPDM}	2.7 MPa
Relaxation time EPDM	τ_{EPDM}	0.5

Table 1: Summary of material properties

The evaluation of the material response contains the resulting horizontal force component at upper end of RVE, see Fig. 3. Futhermore, the Cauchy shear stress distribution at maximum deformation is shown at time $t = 4.5s$, see Fig. 4. Within the force-displacement diagram, the hysteresis effect can be seen after each cyclic load, whereby only slight changes can be observed after the fourth load cycle. The shear stresses are mainly present in the matrix, due to the higher stiffness compared to the filler material.

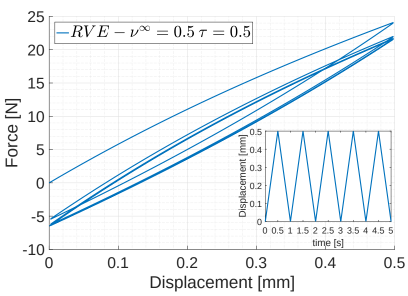

Fig. 3: Material behaviour of EPDM/PP

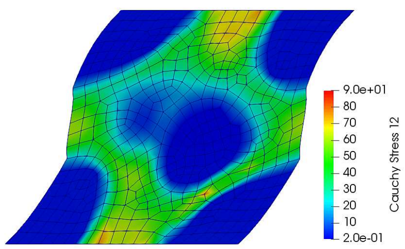

Fig. 4: Shear stress distribution at $t = 4.5s$

Acknowledgements Open access funding enabled and organized by Projekt DEAL.

References

[1] O.C. Zienkiewicz: The Finite Element Method for Solid and Structural Mechanics, (Butterworth-Heinemann, 2014), chap. 6.